SHOCK, Vol. 13, No. 1, pp. 52–59, 2000

OXIDATIVE STRESS PRECEDES CIRCULATORY FAILURE INDUCED BY 35-GHZ MICROWAVE HEATING

John Kalns,*† Kathy L. Ryan,‡§ Patrick A. Mason,*‡ John G. Bruno,‡‖ Robert Gooden,† and Johnathan L. Kiel‡

**Veridian Engineering, Inc. at Brooks AFB, Texas 78235, †Davis Hyperbaric Laboratory, San Antonio, Texas 78235; ‡Air Force Research Laboratory, Directed Energy Bioeffects Division, Brooks AFB, Texas 78235; §Department of Biology, Trinity University, San Antonio, Texas 78212; ‖University of Texas Health Science Center, San Antonio, Texas 78284*

Received 12 Apr 1999; first review completed 26 May 1999; accepted in final form 7 Jul 1999

ABSTRACT—Sustained whole-body exposure of anesthetized rats to 35-GHz radio frequency radiation produces localized hyperthermia and hypotension, leading to circulatory failure and death. The physiological mechanism underlying the induction of circulatory failure by 35-GHz microwave (MW) heating is currently unknown. We hypothesized that oxidative stress may play a role in the pathophysiology of MW-induced circulatory failure and examined this question by probing organs for 3-nitrotyrosine (3-NT), a marker of oxidative stress. Animals exposed to low durations of MW that increased colonic temperature but were insufficient to produce hypotension showed a 5- to 12-fold increase in 3-NT accumulation in lung, liver, and plasma proteins relative to the levels observed in control rats that were not exposed to MW. 3-NT accumulation in rats exposed to MW of sufficient duration to induce circulatory shock returned to low, baseline levels. Leukocytes obtained from peripheral blood showed significant accumulation of 3-NT only at exposure levels associated with circulatory shock. 3-NT was also found in the villus tips and vasculature of intestine and within the distal tubule of the kidney but not in the irradiated skin of rats with MW-induced circulatory failure. The relationship between accumulation in liver, lung, and plasma proteins and exposure duration suggests either that nitro adducts are formed in the first 20 min of exposure and are then cleared or that synthesis of nitro adducts decreases after the first 20 min of exposure. Taken together, these findings suggest that oxidative stress occurs in many organs during MW heating. Because nitration occurs after microwave exposures that are not associated with circulatory collapse, systemic oxidative stress, as evidenced by tissue accumulation of 3-NT, is not correlated with circulatory failure in this model of shock.

KEYWORDS—nitration, peroxynitrite, 3-nitrotyrosine, radio frequency radiation, microwaves, blood pressure

INTRODUCTION

Sustained, whole-body exposure of ketamine-anesthetized rats to 35-GHz radio frequency radiation produces a pattern of heating that is characterized by a pronounced increase in skin temperature at the irradiated site with only moderate heating of the body core (1). This is because the shallow depth of penetration at this frequency (35 GHz) results in the deposition of energy primarily in the cutaneous region (2, 3). Although the degree of core body heating differs from that associated with heat stroke induced by environmental heating, the cardiovascular responses to 35-GHz microwave (MW) heating are remarkably similar to those produced by sustained environmental heat stress (4). That is, both MW heating and environmental heating produce an increase in heart rate. In addition, arterial blood pressure is well maintained during the initial stages of hyperthermia but, as heating continues, blood pressure decreases and eventuates in circulatory failure in both instances. Furthermore, pronounced mesenteric vasodilation accompanies the onset of the hypotensive response in both MW heating and environmental heat stress (1, 4). Thus, MW exposure produces a pattern of cardiovascular responses similar to that produced by a more familiar modality of heating (i.e., environmental heat stress), despite a different thermal distribution.

The identity of primary molecular mediators of MW-induced circulatory failure is not known. Experimental evidence obtained thus far, however, has shown that some pathways are not involved in the pathophysiology of MW-induced hypotension and shock. Nitric oxide (NO) is upregulated during shock of many different etiologies and is thought to play an important role in shock pathogenesis by increasing vasodilation and thereby contributing significantly to vascular collapse (5–7). The importance of NO in contributing to many types of experimental shock has been supported by observations demonstrating that pharmacological inhibition of *de novo* NO synthesis reduces vascular decompensation, increases blood pressure, and ultimately increases survival (5–7). Similar experiments performed in the MW-induced shock model using the NO synthase (NOS) inhibitor N^{ω}-nitro-L-arginine methyl ester (L-NAME) delivered either chronically during a 2-week period before MW exposure (8) or at inhibitory doses administered acutely after MW exposure (9) demonstrate that NOS inhibition has virtually no effect on blood pressure or survival time. These findings suggest that *de novo* synthesis of NO does not contribute to MW-induced circulatory failure. Conversely,

Address reprint requests to John Kalns, Ph.D., USAFSAM/AFI, 2602 West Gate Rd., Brooks AFB, TX 78235.

Report Documentation Page

Form Approved
OMB No. 0704-0188

1. REPORT DATE	2. REPORT TYPE	3. DATES COVERED
01 JAN 2000	**N/A**	**-**

4. TITLE AND SUBTITLE	5a. CONTRACT NUMBER
Oxidative stress precedes circulatory failure induced by 35-GHz microwave heating.	5b. GRANT NUMBER
	5c. PROGRAM ELEMENT NUMBER
6. AUTHOR(S)	5d. PROJECT NUMBER
Kalns J. E., Ryan K. L., Mason P. A., Bruno J. G., Gooden R., Kiel J. L.,	5e. TASK NUMBER
	5f. WORK UNIT NUMBER
7. PERFORMING ORGANIZATION NAME(S) AND ADDRESS(ES)	8. PERFORMING ORGANIZATION REPORT NUMBER
United States Army Institute of Surgical Research, JBSA Fort Sam Houston, TX 78234	
9. SPONSORING/MONITORING AGENCY NAME(S) AND ADDRESS(ES)	10. SPONSOR/MONITOR'S ACRONYM(S)
	11. SPONSOR/MONITOR'S REPORT NUMBER(S)

12. DISTRIBUTION/AVAILABILITY STATEMENT
Approved for public release, distribution unlimited

13. SUPPLEMENTARY NOTES

14. ABSTRACT

15. SUBJECT TERMS

16. SECURITY CLASSIFICATION OF:			17. LIMITATION OF ABSTRACT	18. NUMBER OF PAGES	19a. NAME OF RESPONSIBLE PERSON
a. REPORT	b. ABSTRACT	c. THIS PAGE			
unclassified	**unclassified**	**unclassified**	**SAR**	**8**	

continuous infusion of *S*-nitroso-*N*-acetylpenicillamine (SNAP), an agent producing pharmacologically significant, steady-state levels of NO *in vivo,* during MW exposure has no effect on blood pressure or survival time (10).

Production of highly reactive (relative to NO) and potentially toxic-free radical species occurs during many forms of traumatic injury and shock (11, 12) and an increasingly important role for these compounds in shock pathogenesis is emerging. In hemorrhagic, endotoxic, and splanchnic artery occlusion/reperfusion models of shock induction, levels of peroxynitrite, a toxic-free radical formed *in situ* by the reaction of NO and superoxide, increase within 1 h (13). Furthermore inhibition of peroxynitrite formation prevents both cellular damage and vasodilation after hemorrhage or ischemia/reperfusion (14, 15). Because heme-containing red blood cells are reservoirs of NO (16, 17), *de novo* synthesis may not be a strict requirement for increased levels of free NO if there is chemical motivation for liberation. MW exposure may provide the required chemical motivation for release of NO from red blood cells because exposure to 2450-MHz radio frequency radiation *in vitro* has been shown to increase erythrocyte sensitivity to oxidative hyperthermic hemolysis (18) and to reversibly alter the thermodynamics of oxygen binding to hemoglobin (19). This evidence, albeit indirect, suggests the possibility that NO release may occur from red blood cells as they pass through MW-exposed skin.

These observations have led us to hypothesize that free radicals may act as mediators of the circulatory failure induced by sustained MW exposure. Because the *in vivo* half-life of free radicals is <1 s *in vivo* (11), we measured the abundance of 3-nitrotyrosine (3-NT), a molecule that is produced from the interaction of nitrating free and protein bound tyrosine. We anticipated that, if free radicals were involved as mediators, then 3-NT accumulation would be correlated with shock. In other words, the highest levels of 3-NT are expected after exposures associated with shock and that less accumulation will occur after exposures not associated with shock.

MATERIALS AND METHODS

Animal care

All experiments and animal care procedures were approved by the Institutional Animal Care and Use Committee of Air Force Research Laboratories, Brooks Air Force Base, Texas and were conducted according to the National Institutes of Health "Guide for the Care and Use of Laboratory Animals" prepared by the Committee on Care and Use of Laboratory Animals of the Institute of Laboratory Animal Resources-National Research Council.

Male Sprague-Dawley rats were obtained from the colonies of Charles River Laboratories (Wilmington, MA). They were individually housed in standard plastic cages (26 × 23 × 20.5 cm) with water and food available *ad libitum.* Rats were 4–5 months old and weighed 350–400 g (367 ± 1 g) at the time of the experiments. A 12-h light:12-h dark cycle (light on at 6:00 a.m.) was used, and the room temperature was maintained at 22–24°C.

Instrumentation and preparation

Animals were anesthetized with urethane (1.6 g/kg; i.p.), and left and right abdominal areas were shaved before surgery. Colonic temperature (T_c) was maintained at 37.0 ± 0.5°C during all surgical procedures. A Teflon catheter (PE 20) was placed into a carotid artery for measurement of arterial blood pressure. The catheter was attached to a precalibrated blood pressure transducer (model CP-01; Century, Inglewood, CA). A lead II electrocardiogram (ECG) was obtained with use of nylon-covered fluorocarbon leads attached to a shielded cable placed outside the MW field. All measured variables were recorded continuously throughout experimentation on a Gould TA2000 recorder.

Animals were also instrumented to monitor temperature at four sites: 1) left subcutaneous (lateral, midthoracic, side facing the MW antenna; T_{sl}); 2) left tympanic; 3) colonic (5–6 cm post-anus); and 4) tail (subcutaneous, dorsal, 1 cm from base). The tail was placed within a 4-cm-diameter tube wrapped with 2 layers of radio frequency radiation shielding material (Bekaert Steel Wire Corp., Marietta, GA). Thus, the tail was shielded from direct exposure to MW, yet air was allowed to flow freely around the tail. All temperature measurements were obtained via thermistor probes (BSD Medical Corporation, Salt Lake City, UT) attached to a precision thermometry system (model BSD-200; BSD Medical Corporation). All temperature and cardiovascular data were A/D (analog to digital) converted by an IBM-compatible custom-designed monitoring system with real-time graphics display and data analysis capabilities.

MW equipment

Continuous-wave 35-GHz fields were generated by a Millimeter Wave Exposure System (Applied Electromagnetics, Inc., Atlanta, GA). Irradiation was conducted under far-field conditions with the animal centered along the boresight, 110 cm from the antenna. The incident power density of the field was determined at the exposure site with an electromagnetic radiation monitor (Narda Microwave Corporation, Hauppauge, NY). The generator power output was monitored throughout exposure with a model 4-32-B Hewlett-Packard power meter. Irradiation was conducted in an Eccosorb RF-shielded anechoic chamber at the Radiofrequency Radiation Division of the USAF Armstrong Laboratory, Brooks Air Force Base, Texas. Chamber temperature and relative humidity were maintained at 27.0 ± 0.5°C and 20 ± 5%, respectively, during experimentation.

Experimental procedure

After surgery, the rat was placed on a Plexiglas holder in an anechoic chamber (1). All animals were instrumented with temperature probes (see Instrumentation and preparation) and cardiovascular leads for data collection. After a 10-min control period, the animal was exposed individually in the H orientation (left lateral exposure, long axis of body parallel to magnetic field) to 35-GHz radio frequency radiation at an incident power density of 75 mW/cm^2. The orientation of the animal with respect to the field was previously erroneously reported to be E (e.g., 1); however, cardiovascular and temperature responses to radio frequency radiation at 35 GHz do not differ between E and H orientations (20). This power density results in a whole-body specific absorption rate of 13.0 W/kg (1).

During the 10-min control period, baseline temperatures were recorded, and T_c was maintained at 37.0 ± 0.5°C with use of a water-perfused heating pad. Rats were randomly assigned to 1 of 7 groups (n = 8/group). In the first group, animals were placed on the MW platform and heated with a water-perfused heating pad until T_c = 37.0°C; these rats were not exposed to MWs. In this group, T_c was carefully monitored so that it did not exceed 37.0°C during either surgical or experimental procedures. Rats of the next 4 groups were exposed to MWs until T_c reached a specific temperature (38, 39, 40, or 41°C, respectively). In a sixth group, rats were exposed to MW until mean arterial pressure (MAP) decreased to 75 mmHg. Previous experiments indicated that, if irradiation is discontinued at this point, MAP will continue to decline until death (8–10). Therefore, we discontinued MW exposure at this point and arbitrarily defined this as the point of circulatory shock induction. These animals were pooled in subsequent analysis as a group with T_c = 42+°C, although the T_c at attainment of endpoint was actually 42.7 ± 0.1°C. In a final group, rats were anesthetized and instrumented but were not exposed to MW; this group was maintained at T_c = 37.0 ± 0.5°C and monitored for a total of 55 min as a time control for MW exposure groups. Cardiovascular and temperature parameters were continuously recorded during the control period and throughout the MW or sham exposure period.

Tissue harvest

Immediately after cessation of MW or sham exposure, the animal was disconnected from all probes and leads and removed from the platform. A midline incision was made, and a blood sample was withdrawn by cardiac puncture into a heparinized vacutainer tube. A 1-mL sample of whole blood was then immediately added to 9 mL of fixative (FACS lysing solution; Bec-

ton-Dickson) for processing by flow cytometry. The remaining blood was separated into plasma and cellular constituents by centrifugation; plasma was collected and immediately frozen and stored at −70°C until time of 3-NT enzyme-linked immunosorbent assay (ELISA). After blood collection, samples of liver, lung, intestine, kidney, and samples of the abdominal skin from the left (irradiated) and right (nonirradiated) sides were immediately placed into 10% neutral-buffered formalin. These were later processed into 4-μm sections and mounted onto positively charged slides for immunohistochemistry.

Measurement of 3-NT using flow cytometry

After fixation and lysis, cells were washed 2 times in 10 mL Dulbecco's Phosphate-Buffered Saline (DPBS), blocked with 10% normal goat serum in DPBS for 30 min, centrifuged, and then resuspended in 10 μL of rabbit polyclonal IgG anti-3-NT antibody (Upstate Biotechnology, Lake Placid, NY), diluted 20-fold in DPBS in 10% normal goat serum, and incubated overnight in the dark at 4°C. Cells were then washed 2 times with 1 mL of DPBS, and the cell pellet was resuspended in 10 μL of phycoerythrin-conjugated goat anti-rabbit Fab fragment (Sigma, St. Louis, MO), diluted 20-fold in DPBS, and then incubated for 1 h at room temperature. After incubation, the cells were washed with 1 mL of DPBS and then suspended in 400 μL of DPBS.

Processing for 3-NT-negative control was identical to the above with the exception that immunoglobulin (Ig)G collected from normal rabbit serum (DAKO, Cupertino, CA) was used instead of anti-3-NT IgG antibody. The concentration of rabbit IgG in the negative control was identical to anti-3-NT antibody. During flow cytometry, cells were selected on a dot-plot of linear SSC × linear FSC. The fluorescence intensity associated with phycoerythrin was measured by using the peak height measured for each cell in the FL-2 bandpass filter. The same instrument settings were used during all runs reported. The geometric mean of the population of FL-2 signals was computed with use of Cell Quest software (Becton-Dickinson) and used in subsequent statistical comparisons. A minimum of 10,000 cells was used for population statistics.

Measurement of 3-NT in plasma

A 20-μL sample of plasma was mixed with 80 μL of 0.1 M sodium bicarbonate buffer (pH 8.5) and then placed in a 96-well ELISA plate and allowed to bind for 2 h at 37°C and then overnight at 4°C (21). The sample was then decanted, and the endogenous peroxidase activity neutralized by addition of 0.3% hydrogen peroxide in methanol for 30 min at room temperature in the dark. Nonspecific binding was blocked with 10% Normal Goat Serum (NGS; BioDesign International, Kennebunk, ME) for 1 h at 37°C. Wells were washed 3 times with 10% NGS, 0.05% Tween 20 in phosphate-buffered saline (PBS). After the last wash, 1.6 μg of rabbit 3-NT polyclonal antibody (Upstate Biotechnology) in 100 μL of PBS was added to each well for 1 h at room temperature, decanted, and washed 3 times with 10%NGS/PBS/0.05% Tween 20. Goat-anti rabbit IgG-biotin conjugate (Sigma) 1:2000 in 10% NGS/PBS 100 μL was added to each well for 1 h at 37°C. Wells were washed 2 more times with 10% NGS/PBS/0.05% Tween 20 followed by 1 wash with 10% NGS/PBS. A colorometric signal proportional to the amount of 3-NT was obtained by using an avidin conjugated horseradish peroxidase system (Vector Laboratories, Burlingame, CA). After a 20-min development, the reaction was stopped with addition of 100 μL of 2% sodium dodecyl sulfate (SDS) in deionized water, and absorbance was read at 405 nm on a microtiter plate reader.

Immunohistochemical detection of 3-NT in tissue

Tissue sections were deparaffinized in xylene and then rehydrated. Nonspecific binding was blocked by incubation of sections in 10% NGS in PBS for 1 h followed by incubation with the rabbit polyclonal 3-NT antibody 1:200 for 2 h at room temperature. Slides were then washed 3 times in PBS and then incubated with goat anti-rabbit phycoerythrin conjugate for 1 h at room temperature. Slides were washed in PBS, dried, and coverslips mounted with a antifading agent (Sigma). Images were captured by using an inverted laser-scanning confocal microscope (Carl Zeiss, Inc., Thornwood, NY). Excitation of phycoerythrin was performed by using a 568-nm laser, and the resulting fluorescence was captured by using a 590- to 610-nm band-pass filter. The intensity of the fluorescent signal was measured by using Zeiss Image software. Background fluorescence correction was made by subtracting the signal obtained from an image prepared in the same manner as above with the exception that nonimmune rabbit polyclonal IgG was substituted for the rabbit 3-NT antibody. The concentration of nonimmune IgG was the same as that used for 3-NT antibody, and the image location was identical to that used in 3-NT stained section. Tissue sections exposed to 5 μM of peroxynitrite were used as positive controls, and competitive inhibition of 3-NT antibody binding with free 3-NT (10 μM) and reduction of 3-NT before exposure to 3-NT antibody were used as negative controls.

Data analysis

Means and standard error of means are shown in graphs. The statistical significance of differences between control and MW-exposed animals 3-NT accumulation was determined by using a *post hoc* Tukey Least Significant Difference test. $P < 0.05$ were considered statistically significant.

RESULTS

Table 1 shows the MW exposure times required to obtain either the T_c endpoint or the MAP endpoint (in the 42+ group) in each of the groups. Thermal and cardiovascular responses to MW exposure in the 42+ group are illustrated in Fig. 1. As noted before (1), T_{sl} began to increase at the onset of MW exposure, whereas increases in T_c temporally lagged the T_{sl} increase. Tympanic temperature increases paralleled those of T_c, whereas tail temperature began to increase (indicating tail vasodilation) when T_c reached approximately 37.5°C (data not shown). Heart rate increased continuously throughout the period of MW exposure, reaching the maximum level able to be recorded by our computer system at 42.5 min (Fig. 1). MAP was well maintained during the initial phase of MW exposure, increased dramatically to a peak, and then decreased profoundly. In contrast to previous observations in ketamine- or pentobarbital-anesthetized rats (1, 8–10), the decline in MAP in urethane-anesthetized rats in this study began as T_c approximated 41.5°C, rather than <40°C. Consequently, the MW exposure time required for circulatory failure (as defined by MAP decreasing to 75 mmHg; Table 1) was also longer than in previous studies in ketamine- or pentobarbital-anesthetized rats (1, 8–10).

Exposure to MW increased 3-NT accumulation in liver, kidney, lung, intestine, and connective tissue within the gut, and also in peripheral leukocytes, but not in irradiated (left abdominal) skin. Fig. 2 demonstrates that increased fluorescence intensity, shown as increased brightness, is elevated in livers of all MW-exposed rats and is negligible in non-MW-exposed rats. We validated that the antibody was specific to 3-NT by exposing tissue sections to the 3-NT-specific antibody concurrently with 10 μM of 3-NT. This negative control showed fluorescence intensity that was similar to that of sections exposed to the sham antibody control (micrographs not shown). Furthermore, we exposed tissue sections to the nitrating agent

TABLE 1. **MW exposure times required to attain the T_c or MAP (i.e., MAP = 75) mm Hg for 42+ group) endpoint in each group**

T_c at endpoint (°C)	MW exposure time (min)
38	15.0 ± 3.0
39	24.0 ± 1.5
40	33.7 ± 1.9
41	44.2 ± 1.8
42+ (42.7 ± 0.1)	60.3 ± 2.4

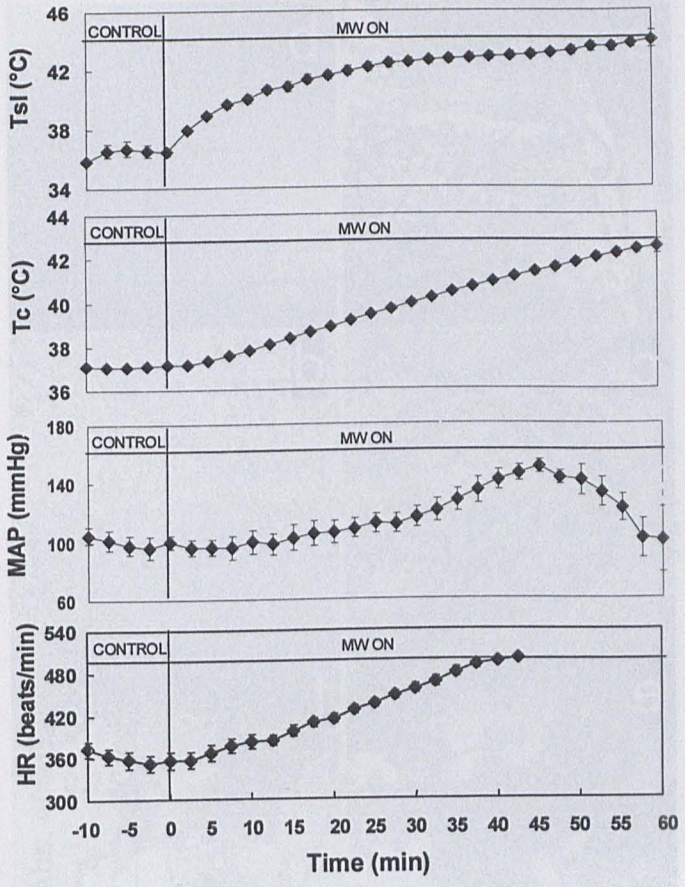

FIG. 1. **Thermal and cardiovascular responses to MW exposure in the group exposed until MAP = 75 mm Hg (i.e., the 42+ group).** T_{sl}, left subcutaneous temperature; T_c, colonic temperature; MAP, mean arterial blood pressure; HR, heart rate.

peroxynitrite (5 μM) for 2 s and compared these with adjacent sections processed in an identical fashion but exposed to the sham antibody. In this case, staining intensity was significantly greater in peroxynitrite-exposed tissue sections stained with the 3-NT antibody. These data show that the procedures that were used here are specific for 3-NT. A similar validation approach was also used in flow cytometric determination of 3-NT accumulation in peripheral leukocytes with similar results.

We also measured and compared the accumulation of 3-NT in liver and lung at various times corresponding to T_c values. To realize this goal, micrographs like those shown in Fig. 2 were converted into pixel maps of brightness or grayscale values. In the case of the liver, a grayscale map was constructed for both a 3-NT-stained section and a sham control prepared from the next tissue section in series. The grayscale pixel maps from 3-NT immunostained and antibody sham control sections were superimposed, and grayscale values of the sham control were subtracted from the tissue section immunostained with the 3-NT specific antibody. For example, the grayscale values corresponding to Fig. 2b were subtracted from the values for Fig. 2a. If there is no accumulation of 3-NT, then the expectation is that the mean grayscale difference is 0. Fig. 3 shows the results of a typical analysis. In the ease of the temperature control (TC), grayscale differences in pixel values range from −30 to 30 with the geometric mean occurring at 2.3, a value

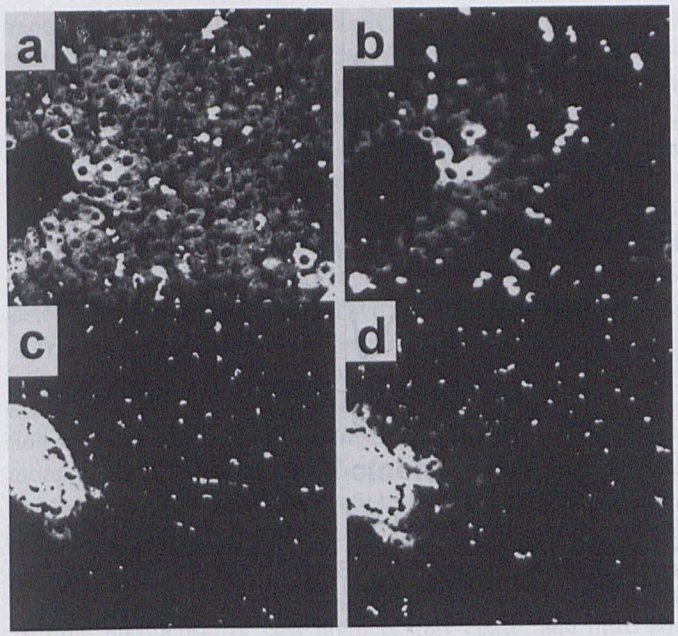

FIG. 2. **Accumulation of 3-NT in the liver of MW-exposed rats.** (a) MW (+), 3-NT Ab(+); (b) MW (+), 3-NT Ab(−); (c) MW(−), 3-NT Ab(+); (d) MW(−), 3-NT Ab(−). Magnification ×630, 590- to 610-nm band-pass filter associated with phycoerythrin. Panels a and b, and panels c and d are serial sections, same location within organ.

that is statistically indistinguishable from 0. In contrast, the values obtained from animals with T_c = 39°C have a range of 10–100 with a mean difference of 45.1. A similar method was used in analysis of tissues obtained from lung.

The relationship between T_c and differences in 3-NT are summarized in Fig. 4. Fig. 4 shows the following: 1) 3-NT is present in lung but not liver of control rats; 2) maximum accumulation of 3-NT occurs at T_cs not associated with circulatory failure, i.e., T_c < 40°C; and 3) 3-NT accumulation is reduced to control levels at T_c > 40°C.

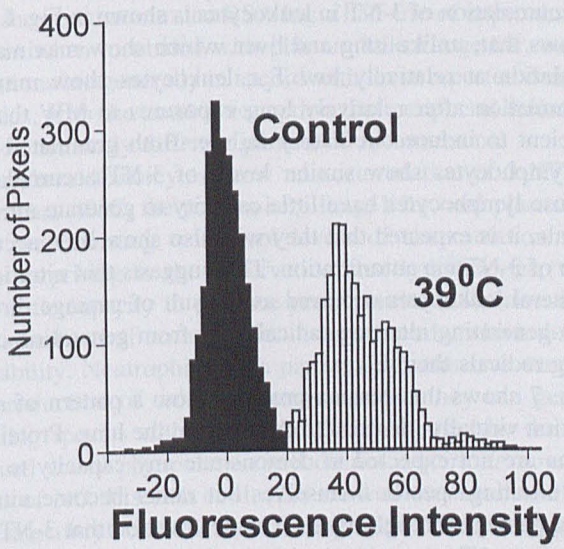

FIG. 3. **Distribution of 3-NT fluorescence in liver.** Relative fluorescence corrected for background. Sum of 10 images taken from 2 rats (20 images total) at each T_c. Geometric mean of each population is represented as a symbol in Fig. 2.

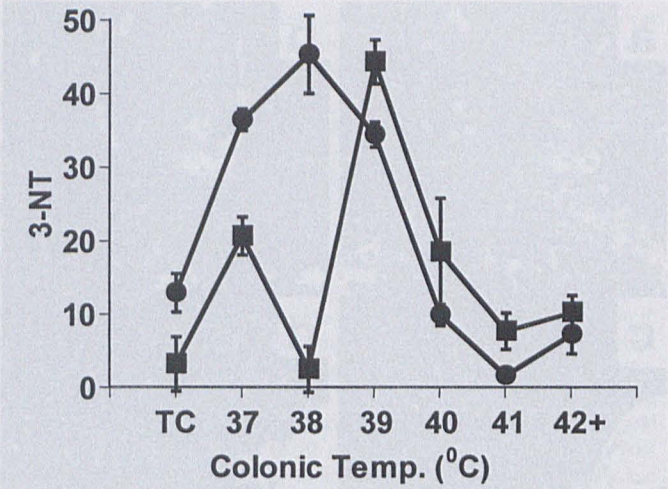

FIG. 4. **3-NT levels in liver and lungs of MW-exposed rats.** Solid circles represent lung tissue; solid squares liver. Each symbol represents mean of 8–10 tissue regions obtained from 2 animals. Values are in relative fluorescence units.

Fig. 5 shows how 3-NT is distributed in various organs after exposure to MW. Significant accumulation of 3-NT occurred within the distal ileum as shown in Fig. 5a. Fig. 5a shows that accumulation was highest in the tips of the villus and on the endothelium of small arteries, suggesting that generation of nitrating compounds occurred directly within these tissues. Fig. 5c shows that accumulation of 3-NT is highest within the cytoplasm of the distal tubule and is not found within the glomerulus or within the endothelium lining the tubule. Because the tubule is a site of extensive amino acid readsorption, we speculate that 3-NT accumulation reflects readsorption of free 3-NT from plasma rather than generation of nitrating radicals within the kidney itself. Fig. 5e and 5f show that 3-NT is uniformly distributed throughout the lung and that control animals also show significant 3-NT accumulation in the lung, an observation that is reflected in Fig. 4.

Accumulation of 3-NT in leukocytes is shown in Fig. 6. Fig. 6 shows that, unlike lung and liver, which show maximal accumulation at relatively low T_cs, leukocytes show maximal accumulation after relatively long exposures to MW that are sufficient to induce circulatory failure. Both granulated cells and lymphocytes show similar levels of 3-NT accumulation. Because lymphocytes have little capacity to generate nitrating radicals, it is expected that they will also show little accumulation of 3-NT via autonitration. This suggests that nitration of peripheral leukocytes occurred as a result of passage through tissue-generating nitrating radicals, not from generation of nitrating radicals themselves.

Fig. 7 shows that plasma proteins show a pattern of accumulation virtually identical to that seen in the lung. Proteins in plasma are not expected to demonstrate any capacity to generate nitrating species themselves but rather become nitrated during passage through tissue. The observation that 3-NT levels decline at T_cs associated with shock induction suggests that nitrate groups present on plasma proteins, or the proteins themselves, are rapidly cleared from the circulation after rapid production during the first 20 min of exposure.

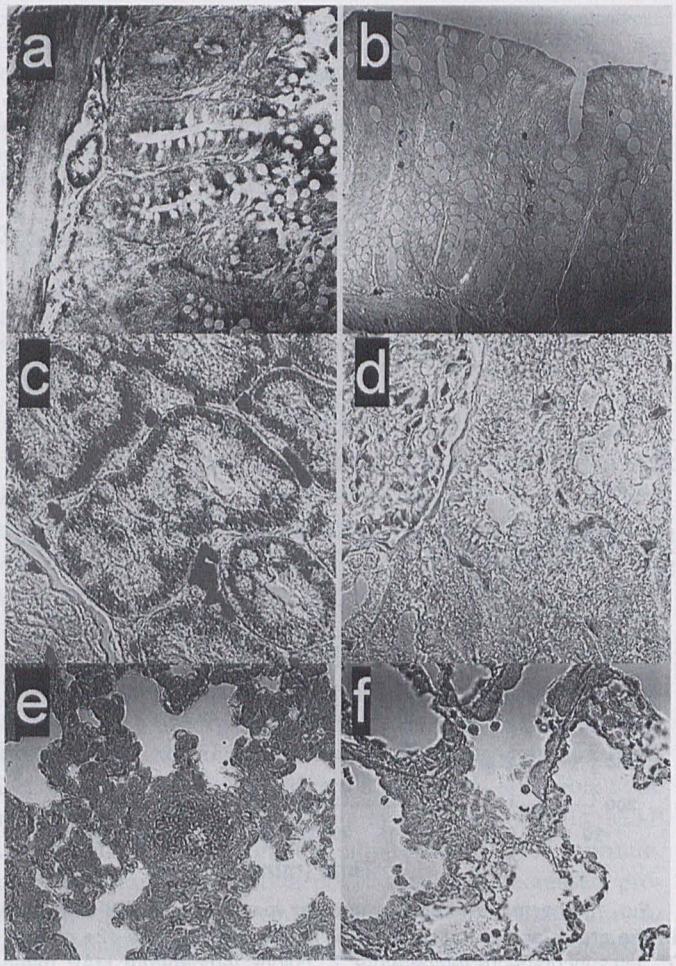

FIG. 5. **Distribution of 3-NT in tissue after exposure to MW.** Transmitted light image overlaid with image from 490- to 510-nm bandpass filter corresponding 3-NT. (a) Distal ileum of rat with final T_c = 42.7°C (i.e., in MW-induced shock). (b) Same region in sham control. (c) Kidney of rat with final T_c = 42.7°C. Glomerulus in lower left hand corner; bright red areas in interstitial spaces between tubules are red blood cells. (d) Sham control. Bright spots are red blood cells; glomerulus shown in upper right hand corner. (e) Lung tissue in animal with final T_c = 39°C (nonshock) showing uniform distribution of 3-NT. (f) Sham control showing positive staining though at only 30% the intensity of MW-exposed rat. Panels c and d, ×1000; all others ×630.

DISCUSSION

The production of nitrating radicals and subsequent accumulation of 3-NT occurs during models of shock arising from various physiological insults. Our findings are unique because MW-induced shock is not associated with significant blood loss or extensive trauma (22). Examination of previous reports about shock produced by other insults, particularly hemorrhage shock, is informative because it demonstrates that MW-induced circulatory failure is not unique for underlying pathology, but rather shares many common aspects. Szabó et al. (13) showed that hemorrhage to a blood pressure of 50 mmHg produces a 9-fold increase in peroxynitrite within 1 h, demonstrating that nitrating species are generated very rapidly during the early phase of shock. Inhibition of *de novo* NO synthesis by L-NAME reduced peroxynitrite production to levels observed in control conditions (13), suggesting that *de novo* synthesis is important in the generation of nitrating radicals during hem-

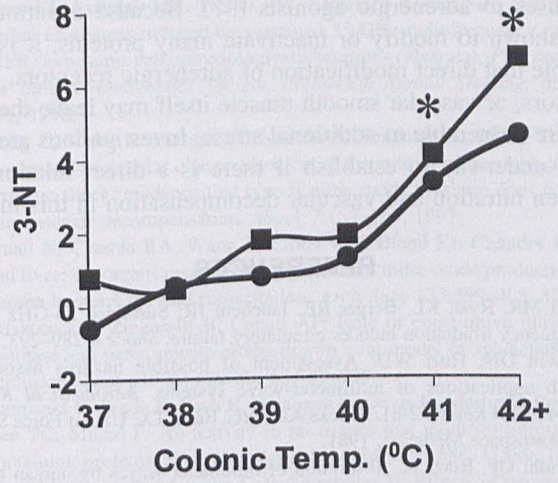

FIG. 6. **3-NT levels in lymphocytes and neutrophils after MW exposure.** Solid circles represent lymphocytes; solid squares represent neutrophils. Each symbol is the mean value of 5–8 rats. Values are in relative fluorescence units.

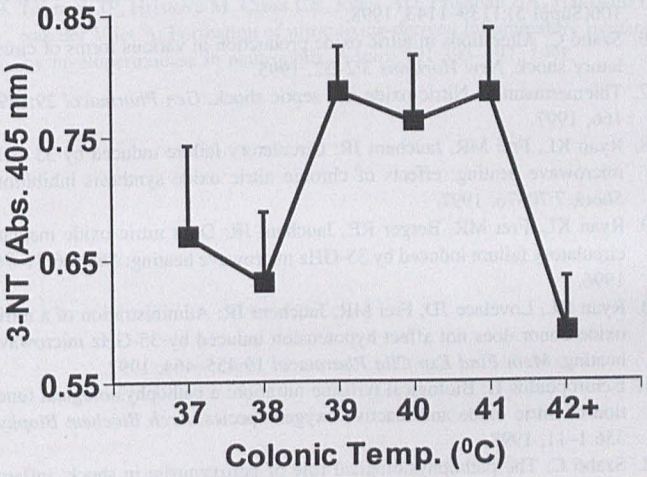

FIG. 7. **3-NT levels in plasma.** Solid squares represent mean of 6–8 rats.

orrhagic shock. It is unclear from the results that we have obtained herein whether administration of L-NAME would alter tissue distribution of 3-NT after MW exposure, although it is clear from previous work that L-NAME does little to alter either the decrease in blood pressure or the time course of circulatory failure following MW exposure (8, 9). The relationship between NOS inhibition, 3-NT accumulation, and hemodynamic instability is currently under investigation.

The source of NO produced during hemorrhagic shock is still far from clear; however, our observations of MW-induced shock are consistent with the current knowledge about this question. Constitutive, endothelial NOS messenger ribonucleic acid (mRNA) and protein were not found to be upregulated in either the liver or the lung following hemorrhagic shock (23). In this case (23), plasma nitrate/nitrite levels were not affected, but nitrosylated hemoglobin increased, suggesting that liberation of NO from some source did occur. This finding suggests that *de novo* synthesis of NO is not a strict requirement for nitration to occur in hemorrhagic shock and, by extension, in other models of shock such as that induced by sustained MW exposure. In a similar hemorrhagic shock model, Smail et al. (24) showed that plasma nitrate/nitrite levels increased approximately 4-fold in shock versus nonshock controls 1.5 h after induction and approximately 12-fold at 4 h. Furthermore, concentrations of nitrate/nitrite at 4 h in liver and intestine were found to be 3- and 4-fold greater, although levels in the kidney were not significantly increased. In a model of splanchnic artery occlusion shock (25), distal ileum was necrotic and stained positively for 3-NT 1 h after reperfusion, a result that is consistent with MW exposure that we observed.

We observed that oxidative stress, as indicated by accumulation of 3-NT in the liver and the lung, occurs after MW exposures that are not associated with vascular decompensation and shock, i.e., exposures resulting in $T_c < 40°C$. Furthermore, maximal accumulation occurs at 38–39°C with decline to near baseline levels as exposure time and T_c increase further. One possible explanation for this phenomenon is that oxidative stress in these organs occurs within the first 20 min of MW exposure, resulting in a buildup of 3-NT. After approximately 20 min, production of new adducts may cease, and nitro adducts are removed so that, at longer exposures (and higher T_c), levels of 3-NT in these organs return to baseline levels. In support of this hypothesis is the finding of Kamisaki et al. (26) who showed that 3-nitro adducts to tyrosine in bovine serum albumin (BSA) have a half-life of approximately 10 min when incubated with rat spleen or lung homogenates. This report also showed that liver and kidney have virtually no ability to remove 3-nitro adducts from BSA. Pretreatment of rats with endodotoxin increased clearance of 3-nitro adducts, suggesting that denitration mechanisms are inducible (26). Because little is now known about "denitrase" activity, regulation, or specificity, it is possible that a denitrase enzyme present in the liver may have negligible activity toward nitrated BSA but may have high activity against nitrated proteins found in the liver after exposure to MW. The finding that plasma proteins show a pattern of nitration buildup and decline similar to that observed in lung is supported by the findings of Gow et al. (27) who showed that nitrated BSA has a half-life of approximately 15 min when incubated with plasma. Taken together, our observations are generally in accord with these reported denitrase kinetics, with the notable exception that peripheral leukocytes show a distinctly different pattern of accumulation.

Peripheral leukocytes show no accumulation of 3-NT until T_c reaches 40°C, the point where lung, liver, and plasma proteins are returning to control levels of accumulation. Even more surprising is the observation that lymphocytes, which have little capacity to produce peroxynitrite (28), have nearly the same level of accumulation as neutrophils, which do have this ability. Neutrophils are a particularly attractive candidate for production of oxidative stress because they can generate nitrating species within the time limits imposed by the MW-induced shock phenomenon and do not require *de novo* synthesis of NO. Eiserich et al. (29) showed that neutrophils can generate nitryl chloride, a nitrating and chlorinating radical formed from hydrogen peroxide, and physiological levels of nitrate. Because neutrophils have also been implicated in ischemic injury, we had initially hypothesized that they may play an important role in MW-induced shock. Peripheral neutro-

phils did show significant levels of 3-NT after exposures associated with shock, and slight accumulation of neutrophils was observed in colon (not shown). However no neutrophils were noted in liver and lung after MW exposure not associated with shock, i.e., <40°C. Taken together, these data suggest that activated neutrophils are not responsible for the extensive tissue accumulation of 3-NT observed.

It should be noted that blood pressure began to decrease in this study using urethane-anesthetized rats occurred at $T_c \geq 41.5$°C and at longer exposure times than in previous studies. For example, MAP first began to decrease when T_c exceeded 37.5°C in ketamine-anesthetized rats (1). Furthermore, the onset of circulatory failure (as defined by MAP decreasing to 75 mmHg) in this study occurred at 42.7 ± 0.1°C; in previous studies using either ketamine- or pentobarbital-anesthetized rats, the onset of circulatory failure occurred at T_cs approximating 40°C (8–10). Indeed, death produced by continuous MW exposure occurred at $T_c \leq 42$°C in ketamine-anesthetized rats (1, 30). In each of these previous instances, MW exposure produced a much more pronounced difference between T_{sl} and T_c than that observed in the current study. Because the exposure parameters used in all of these experiments were identical, it is probable that the difference in temperature distribution and consequent timing of the hypotensive response is due to the use of urethane anesthesia rather than either ketamine or pentobarbital. Urethane was used in this study because, concurrently with taking blood and tissue samples for nitrated protein analysis, blood and brain samples were simultaneously taken for analysis of catecholamine content (data not reported herein); the use of urethane is common and well accepted for determination of catecholamine levels (31, 32). The mechanism underlying the effect of urethane anesthesia on the relationship between T_c and the development of hypotension during MW exposure is not well understood. It is interesting to note that, whatever the mechanism, the increased levels of T_c attained before hypotension ensues correspond to the levels of T_c required to produce hypotension and heat stroke by environmental heating. That is, MAP begins to decrease at $T_c > 41.5$°C in conscious (4), chloralose-anesthetized (4), or urethane-anesthetized (33) rats when exposed to prolonged heat stress. Whether accumulation of 3-NT in tissues of animals exposed to environmental heat stress is also increased is not known but is worthy of further study.

MW exposure induces a burst of oxidative stress that results in extensive nitration in tissues far removed from the site of MW exposure. The transient accumulation of 3-NT appears to be unrelated to vascular collapse because maximal accumulation occurs after exposures insufficient to produce shock. This does not strictly rule out the possibility that nitrating radicals contribute to this model of shock induction. Peroxynitrite has been shown to increase levels of cyclic guanosine monophosphate in smooth muscle, suggesting that nitration may lead to vasodilation and thus contribute to hypotension (34). If liberated in sufficient quantities, 3-NT may also reduce the effect of epinephrine and other adrenergic agonists (35) and attenuate the vascular response to angiotensin II (36), phenomena that might be expected to contribute to vascular decompensation. Recently, peroxynitrite has also been shown to attenuate vascular responses to adrenergic agonists (37). Because nitration has been shown to modify or inactivate many proteins, it is also possible that direct modification of adrenergic receptors, other receptors, or vascular smooth muscle itself may leave the vasculature vulnerable to additional stress. Investigations are currently underway to establish if there is a direct relationship between nitration and vascular decompensation in this model.

REFERENCES

1. Frei MR, Ryan KL, Berger RE, Jauchem JR: Sustained 35-GHz radiofrequency irradiation induces circulatory failure. *Shock* 4:289–293, 1995.
2. Erwin DN, Hurt WD: Assessment of possible hazards associated with applications of millimeter-wave systems. *Aeromedical Review USAFSAM Review* 2-81. Brooks Air Force Base, TX: US Air Force School of Aerospace Medicine, 1981.
3. Gandhi OP, Riazi A: Absorption of millimeter waves by human beings and its biological implications. *IEEE Trans Microwave Theory Tech* 34: 228–235, 1986.
4. Kregel KC, Wall PT, Gisolfi CV: Peripheral vascular responses to hyperthermia in the rat. *J Appl Physiol* 64:2582–2588, 1988.
5. Shah NS, Billiar TR: Role of nitric oxide in inflammation and tissue injury during endotoxemia and hemorrhagic shock. *Environ Health Perspect* 106(Suppl 5):1139–1143, 1998.
6. Szabó C: Alterations in nitric oxide production in various forms of circulatory shock. *New Horizons* 3:2–32, 1995.
7. Thiemermann C: Nitric oxide and septic shock. *Gen Pharmacol* 29:159–166, 1997.
8. Ryan KL, Frei MR, Jauchem JR: Circulatory failure induced by 35 GHz microwave heating: effects of chronic nitric oxide synthesis inhibition. *Shock* 7:70–76, 1997.
9. Ryan KL, Frei MR, Berger RE, Jauchem JR: Does nitric oxide mediate circulatory failure induced by 35-GHz microwave heating: *Shock* 6:71–76, 1996.
10. Ryan KL, Lovelace JD, Frei MR, Jauchem JR: Administration of a nitric oxide donor does not affect hypotension induced by 35-GHz microwave heating. *Meth Find Exp Clin Pharmacol* 19:455–464, 1997.
11. Ischiropoulos H: Biological tyrosine nitration: a pathophysiological function of nitric oxide and reactive oxygen species. *Arch Biochem Biophys* 356:1–11, 1998.
12. Szabó C: The pathophysiological role of peroxynitrite in shock, inflammation, and ischemia-reperfusion injury. *Shock* 6:79–88, 1996.
13. Szabó C, Salxman AL, Ischiropoulos H: Peroxynitrite-mediated oxidation of dihydrorhodamine 123 occurs in early stages of endotoxic and hemorrhagic shock and ischemia-reperfusion injury. *FEBS Lett* 372:229–232, 1995.
14. Cuzzocrea S, Zingarelli B, Costantino G, Szabó A, Salzman AL, Caputi AP, Szabo C: Beneficial effects of 3-aminobenzamide, an inhibitor of poly (ADP-ribose) synthetase in a rat model of splanchnic artery occlusion and reperfusion. *Br J Pharmacol* 121:1065–1074, 1997.
15. Szabó C: Potential role of the peroxynitrate-poly(ADP-ribose) synthetase pathway in a rat model of severe hemorrhagic shock. *Shock* 9:341–344, 1998.
16. Butler AR, Megson IL, Wright PG: Diffusion of nitric oxide and scavenging by blood in the vasculature. *Biochim Biophys Acta* 1425:168–176, 1998.
17. Lancaster JR Jr: Simulation of the diffusion and reaction of endogenously produced nitric oxide. *Proc Natl Acad Sci USA* 91:8137–8141, 1994.
18. Kiel JL, Erwin DN: Microwave and thermal interactions with oxidative hemolysis. *Physiol Chem Phys Med NMR* 16:317–323, 1984.
19. Kiel JL, Erwin DN: Microwave radiation effects on the thermally driven oxidase of erythrocytes (1986). *Int J Hyperthermia* 2:201–212, 1986.
20. Frei MR, Jauchem JR, Welch M: Physiological effects of whole-body exposure to millimeter waves (abstract). *Proceedings of the Twelfth Annual Meeting of the Bioelectromagnetics Society,* pp. 87–88, 1990.
21. Bruno JG, Parker JL, Kalns J, Darcy TJ, Grubbs TR, Cox AB, Morales PJ, Alls JL, Kiel JL: Characterization of $NR10_2$ macrophages. *In Vitro Cell Develop Biol (Animal)* 34:613–616, 1998.

22. Ryan KL, Tehrany MR, Trotter RW, Escarciga R, Frei MR, Jauchem JR: Lethal heat stress induced by sustained 35-GHz radiofrequency radiation (RFR) exposure: pathophysiological alterations (abstract). *Proceedings of the Bioelectromagnetics Society, Eighteenth Annual Meeting,* pp. 232–233, 1996.
23. Kelly E, Nishit S, Morgan N, Watkins S, Peitzman A, Billiar T: Physiologic and molecular characterization of the role of nitric oxide in hemorrhagic shock: evidence that type II nitric oxide synthase does not regulate vascular decompensation. *Shock* 7:157–163, 1997.
24. Smail N, Catania RA, Wang P, Cioffi WG, Bland KI, Chaudry IH: Gut and liver: the organs responsible for increased nitric oxide production after trauma-hemorrhage and resuscitation. *Arch Surg* 133:399–405, 1998.
25. Cuzzocrea S, Zingarelli B, Caputi AP: Role of constitutive nitric oxide synthase and peroxynitrite production in a rat model of splanchnic artery occlusion shock (1998) *Life Sci* 63:789–799.
26. Kamisaki Y, Wada K, Bian K, Balabanli B, Davis K, Martin E, Behbod F, Lee YC, Murad F: An activity in rat tissues that modifies nitrotyrosine-containing proteins. *Proc Natl Acad Sci USA* 95:11584–11589, 1998.
27. Gow AJ, Duran D, Malcolm S, Ischiropoulos H: Effects of peroxynitrite-induced protein modifications on tyrosine phosphorylation and degradation. *FEBS Lett* 385:63–66, 1996.
28. Gagnon C, Leblond FA, Filep JG: Peroxynitrite production by human neutrophils, monocytes and lymphocytes challenged with lipopolysaccharide *FEBS Lett* 431:107–110, 1998.
29. Eiserich JP, Hristova M, Cross CE, Jones AD, Freeman BA, Halliwell B, van der Vliet A: Formation of nitric oxide-derived inflammatory oxidants by myeloperoxidase in neutrophils. *Nature* 391:393–397, 1998.
30. Ryan KL, Walters TJ, Tehrany MR, Lovelace JD, Jauchem JR: Age does not affect thermal and cardiorespiratory responses to microwave heating in calorically restricted rats. *Shock* 8:55–60, 1997.
31. Dev BR, Mason PA, Freed CR: Drug-induced changes in blood pressure lead to changes in extracellular concentrations of epinephrine, dihydroxyphenylacetic acid, and 5-hydroxyindoleacetic acid in the rostral ventrolateral medulla of the rat. *J Neurochem* 58:1386–1394, 1992.
32. Dev BR, Nandakumaran M, Philip L, John SJ: Brain natriuretic peptide-mediated changes in the extracellular neurotransmitter turnover in the rostral ventrolateral medulla. *Neuroscience* 84:255–262, 1998.
33. Lin MT, Kao TY, Jin YT, Chen CF: Interleukin-1 receptor antagonist attenuates the heat stroke-induced neuronal damage by reducing the cerebral ischemia in rats. *Brain Res Bull* 37:595–598, 1995.
34. Tarpey MM, Beckman JS, Ischiropoulos H, Gore JZ, Brock TA: Peroxynitrite stimulates vascular smooth muscle cell cyclic GMP synthesis. *FEBS Lett* 364:314–318, 1995.
35. Kooy NW, Lewis SJ: Nitrotyrosine attenuates the hemodynamic effects of adrenoceptor agonists in vivo: relevance to the pathophysiology of peroxynitrite. *Eur J Pharmacol* 310:155–161, 1996.
36. Kooy NW, Lewis SJ: The peroxynitrite product 3-nitro-L-tyrosine attenuates the hemodynamic responses to angiotensin II in vivo. *Eur J Pharmacol* 315:165–170, 1996.
37. Benkusky NA, Lewis SJ, Kooy NW: Peroxynitrite-mediated attenuation of α- and β-adrenoceptor agonist-induced vascular responses in vivo. *Eur J Pharmacol* 364:151–158, 1999.